

# Energy Management that Generates Hopping. Comparison of Virtual, Robotic and Human Bouncing.

Karl Theodor Kalveram <sup>1,2</sup>, Daniel Häufle <sup>3,2</sup>, Sten Grimmer <sup>2</sup>, André Seyfarth <sup>2</sup>

<sup>1</sup> Cybernetical Psychology, University of Duesseldorf, Universitaetsstr.1,  
40225 Duesseldorf, Germany.

<sup>2</sup> Lauflabor Locomotion Laboratory, University of Jena, Dornburger Str. 23,  
07743 Jena, Germany.

<sup>3</sup> Institute of Sport and Movement Science, University of Stuttgart, Allmandring 28,  
70569 Stuttgart, Germany.

kalveram@uni-duesseldorf.de, daniel.haeufle@inspo.uni-stuttgart.de,  
sten.grimmer@uni-jena.de, oas@uni-jena.de

**Abstract:** To get insight into the energy management applied in human hopping, the Marco hopper robot is used to verify different concepts of energy supply. In “constant energy supply”, in each jump -regardless of perturbations- the same amount of mechanical energy is injected, whereas the limitation of hopping height is left to energy dissipation. This induces continuous and robust “terrain following hopping”. It is an example of *exploitive actuation*, which does not rely on feedforward or negative feedback control schemes. In contrast, in “lost energy supply” the mechanical energy that is going to be dissipated in the current cycle is assessed and replaced. This is expected to lead to “apex preserving hopping”, which characterizes the hopping behavior of the spring-loaded inverted pendulum (SLIP). In reality, however, stability seems not achievable by this method. To check, which of the envisaged types of bouncing actuation is nearest to human hopping, we propose to follow the "test trilogy", that is to say, to apply simulation tests, hardware tests and behavioral comparison tests.

**Keywords:** Stable hopping, exploitive actuation, energy management, SLIP model.

## 1 Introduction

Theoretically, the simplest hopper would be a spring-mass arrangement. On landing, the spring slows the body down and stores its kinetic energy as potential energy, and uses the stored energy for the body's subsequent push off. The spring-loaded inverted pendulum (SLIP) <sup>1</sup> is an often-cited example of such a concept. The SLIP models an energetically conservative system, which loses no energy and, therefore, needs no energy replenishment. If confined to vertical motion, the SLIP model exhibits stable hopping in the sense that the apex height, measured absolutely,

remains constant regardless of the distance to ground, even if the terrain varies in altitude. Hence we call this behavior “apex-preserving hopping”. Human hopping, however, requires like other continued real world processes to replenish lost energy and to rule out unpredictable perturbations. Can an energy management complete the SLIP model, such that these requirements are fulfilled?

In engineering, robotic movements are usually generated by negative feedback control and/or feedforward control. In these classical control approaches, motors enforce the joints to attain desired angular trajectories. Examples are Asimo (Honda), Qurio (Sony), or Johnnie (TU Munich). These machines, however, do not specify the motion related energy. They assume that mechanical energy is available if needed. It may be doubted whether this approach is applied in human movement generation.

The SLIP-model, in contrast, operates without such control mechanisms. It rather considers movements as emerging from „exploitive actuation“<sup>2,3</sup>. This denotation includes that a superordinate controller exploits the physics of its own "body" to achieve specified goals like “moving forward until a given location is reached” with - compared to classical control solutions - minimal computational effort. Besides of ignoring the problem how to manage the "lost energy supply", the SLIP model also overlooks the phenomenon that locomotion related biological bouncing is really a “terrain-following hopping”. Hereby, the hopper pursues to keep the distance between apex height and ground profile constant, and not the absolute hopping height.

Looking at existing hopping machines that successfully operate for lots of periods<sup>4-6</sup> reveals, that they leave open whether the machines address apex preserving or terrain following hopping, because the experimental design lacks ground level changes. We conceive that “constant energy supply” will induce “terrain following hopping”. Thereby, in each jump -regardless of perturbations- the same amount of mechanical energy is injected, whereas the limitation of hopping height is left to energy dissipation. On the other hand, “lost energy supply” will lead to “apex preserving hopping”. Here the mechanical energy that is going to be dissipated in the current cycle is assessed and replenished. The question then is, which of both types of energy management is prevalent in human hopping?

To tackle this question, we follow the test trilogy<sup>2</sup>, which incorporates the simulation test, the hardware test, and the behavioral comparison test. According to this test trilogy, a **simulation test** probes whether a concept is mathematically well defined and theoretically sound. A **hardware test** employs a machine (robot) to check whether a successfully simulated theoretical concept is practicable also under real world conditions. A **behavioral comparison test** compares human data to simulated data - generated by a checked model - with respect to the reactions to a perturbation.

## 2 Method

The method comprises the "cascaded damped spring-mass" concept (CDSM model) for hopping, its simulation, the Marco hopper robot as the related hardware, and a preliminary behavioral comparison test.

### 2.1 The Simulation Test of the Hopping Concept

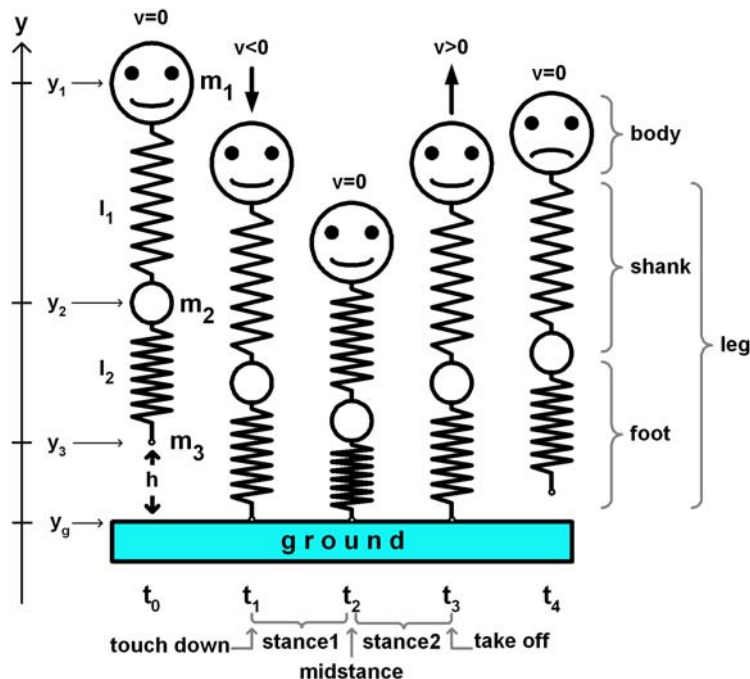


**Figure 1:** Cascaded damped spring-mass model with two segments. The hopper model consists of three point masses  $m_1$ ,  $m_2$ , and  $m_3$  drawn as circles. Between the masses spring-damper elements with lengths  $l_1$ ,  $l_2$  are placed, which have rest lengths  $l_{10}$ ,  $l_{20}$ , stiffness coefficients  $k_1$ ,  $k_2$ , coefficients of viscous damping  $b_1$ ,  $b_2$ , and coefficients of friction  $c_1$ ,  $c_2$ . Mass  $m_1$  is ascribed to the body, and mass  $m_2$  to the shank. Mass  $m_3$  ascribed to the foot is assumed as negligible.  $y_1$ ,  $y_2$ ,  $y_3$  denote the actual vertical positions of the masses,  $y_g$  the position of the ground (floor), and  $y_{COM}$  (not shown) the position of the center of mass (COM). The velocity of the COM is indicated by  $v$ . Midstance is defined as that moment where  $v$  inverts the direction from negative to positive.  $t_2$  denotes the instant where  $l_1$  reaches its minimal length,  $l_{1min}$ , which can slightly deviate from midstance because of the combined compliance of both involved springs. In the following, we disregard from this complication.  $y(0)$  indicates the start height (of  $m_1$  respectively the COM) when the hopper is released, and  $h$  the distance of  $m_3$  to ground level at release. Displayed are five snapshots at time points  $t_0$ ,  $t_1$ ,  $t_2$ ,  $t_3$ ,  $t_4$  within a full stance/flight cycle (fig.1 modified from <sup>2</sup>).

The simulation is based on the CDSM model, which is outlined in detail in fig.1. According to fig.1, spring lengths and velocities of shortening/lengthening of the springs are defined as

$$l_1 = y_1 - y_2, \dot{l}_1 = \dot{y}_1 - \dot{y}_2$$

$$l_2 = y_2 - y_3, \dot{l}_2 = \dot{y}_2 - \dot{y}_3$$

The equations of motion derived from the Lagrange algorithm are

$$m_1 \ddot{y}_1 + m_1 g - k_1(l_{10} - l_1) + b_1 \dot{l}_1 + c_1 \text{sign}(\dot{l}_1) - f_1 = 0$$

$$m_2 \ddot{y}_2 + m_2 g + k_1(l_{10} - l_1) - b_1 \dot{l}_1 - c_1 \text{sign}(\dot{l}_1) + f_1 - k_2(l_{20} - l_2) + b_2 \dot{l}_2 + c_2 \text{sign}(\dot{l}_2) - f_2 = 0$$

$$m_3 \ddot{y}_3 + m_3 g + k_2(l_{20} - l_2) - b_2 \dot{l}_2 - c_2 \text{sign}(\dot{l}_2) + f_2 - f_g = 0$$

$f_1$  and  $f_2$  refer to amendatory extra forces added from within the subsystems, for example by actuators located beneath the masses and acting upon the respective springs.  $f_g$  denotes the ground reaction force that pushes the lower end of the foot spring upwards. If  $m_3$  is neglected, one gets

$$f_g = k_2(l_{20} - l_2) - b_2 \dot{l}_2 - c_2 \text{sign}(\dot{l}_2) + f_2$$

The sign of the ground reaction force  $f_g$  characterizes flight and stance of the spring system:

$$f_g = \begin{cases} = 0 & \text{during flight (or swing)} \\ > 0 & \text{during stance} \end{cases}$$

Assuming an infinitely stiff floor, it holds during stance

$$\ddot{y}_3 = 0, \dot{y}_3 = 0, y_3 = y_g$$

To inject a predetermined portion  $\Delta W$  of potential energy, we configured the amendatory force  $f_1$  of the shank spring as

$$f_1 = \frac{6 \cdot \Delta W}{(l_{10} - l_{1\min})^3} \cdot (l_1 - l_{1\min}) \cdot (l_{10} - l_1)$$

This force is always non-negative, different from zero only between midstance and take off, and can also be generated through an - albeit sliding - stiffness enhancement  $\Delta k_1$  to be added to  $k_1$  during stance 2:

$$\Delta k_1 = \frac{6 \cdot \Delta W}{(l_{10} - l_{1\min})^3} \cdot (l_1 - l_{1\min})$$

In **constant energy supply**, a fixed amount  $\Delta W$  of mechanical energy is put into the system applying the above formula. **Lost energy supply** can be achieved by subtracting the total energy at midstance from the total energy at touch down, and by supplying about twice of this difference using the above formula.

Fig.2 (left column) visualizes the results using Poincaré apex return maps<sup>7,8</sup>. From the simulated movements we extracted the  $y$ -coordinates  $y(i)$  of eight consecutive apices of mass  $m_1$  (body), which were plotted as points  $[y(i), y(i+1)]$ ,  $i=0,1,\dots,8$ . Regarding **constant energy supply**, the points belonging to a given supplied energy converged, closely along the respective dotted line, to a definite place on the bisection line. This indicates that the apex height tends to track the floor profile at a distance determined by  $\Delta W$ . Regarding **lost energy supply**, such a convergence was hard to achieve. Instead of, the points tended to drift away, was indicates that stability could not be upheld.

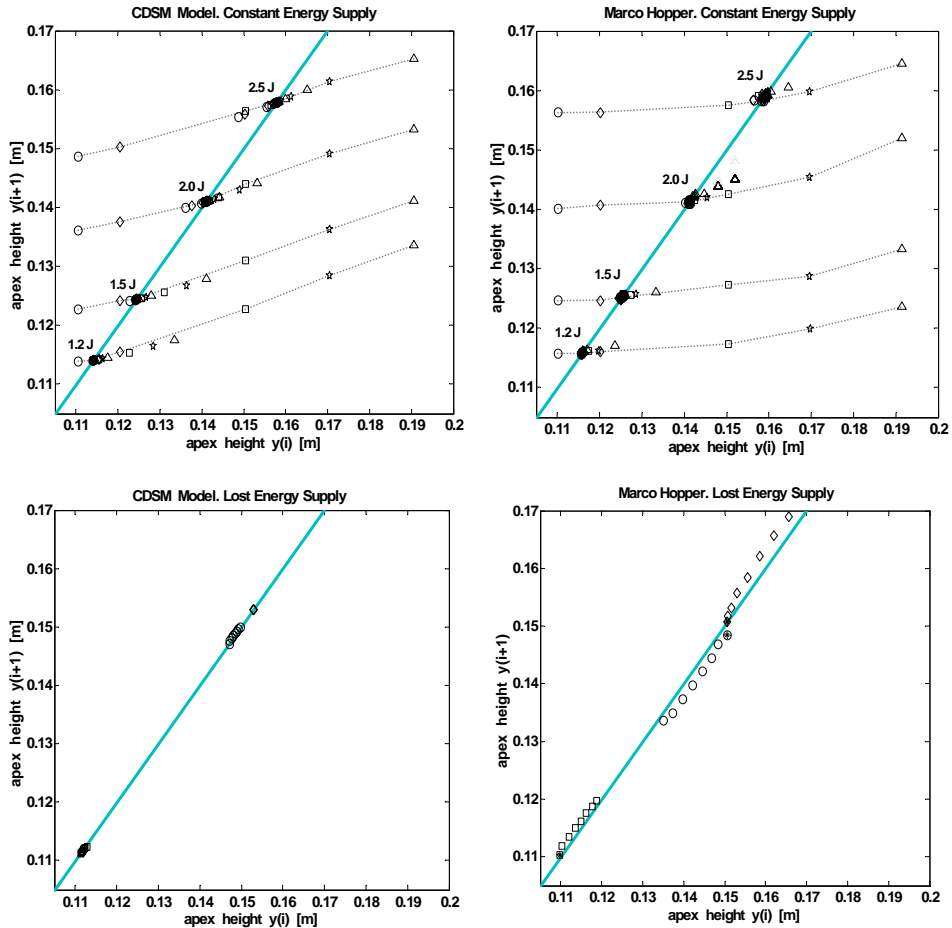


**Figure 2:** Apex return maps produced by the CDSM model (**left column**) and the Marco hopper robot (**right column**), using constant energy supply (**upper row**) or lost energy supply (**lower row**). In **constant energy supply**, the portions of energy supplied were 1.2, 1.5, 2.0 and 2.5J. The release heights  $y(0)$  were 0.11, 0.12, 0.15, 0.17 and 0.19m. Each hopping sequence consisted of eight jumps. The points of a sequence that started from a certain release height are marked with the same labels. In **lost energy supply**, the release heights were 0.112, 0.148 and 0.152m. Theoretically, in each jump the release height should be re-attained, such that the respective points coincide into one point on the bisection line. In fact, however, this held only for the 0.152m release, and only with a carefully adjusted energy supply. With the same adjustment, at the other two supplies the apices drifted away closely along the bisection line.

## 2.2 The hardware test

The Marco (**M**echanical **a**djustable **r**eflexive-**c**ompliant) hopper used for the test is a robot test bed built to investigate the effectiveness of different forcing functions

applied to the leg of a device capable of hopping. Since its first introduction<sup>9</sup> the Marco<sup>a</sup> hopper robot has been modified several times. The version used in the current investigation is illustrated in fig. 3.

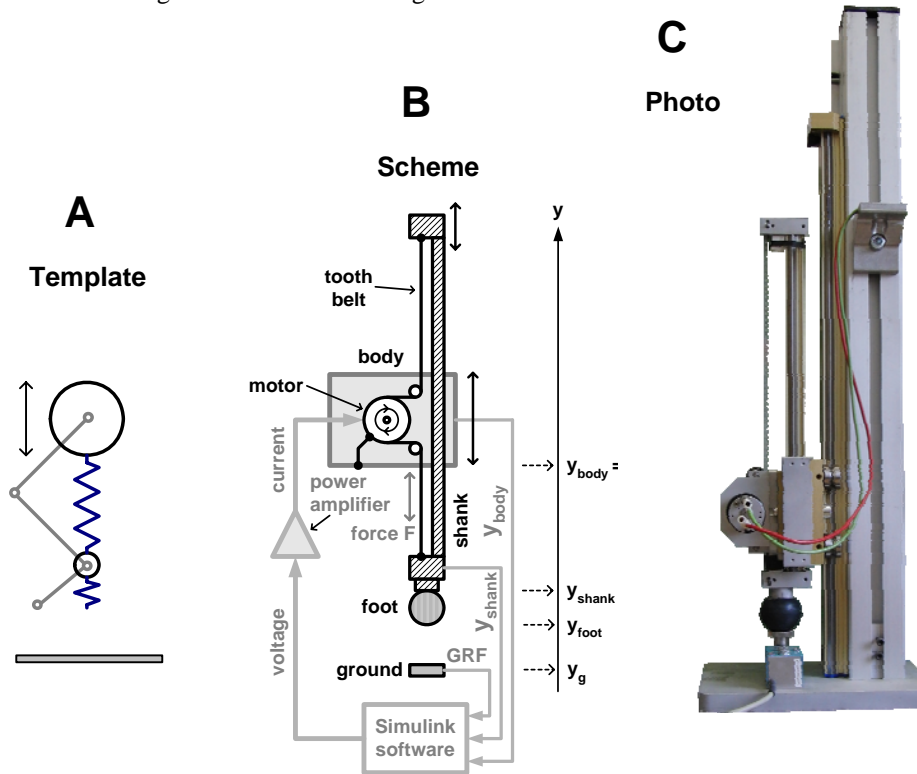


**Figure 3:** The cascaded damped spring-mass model **A** is the template (see fig.1) for the Marco hopper robot, the home position of which is shown in **C**, and its functional scheme in **B**.

The Marco hopper comprises a 1.424kg sledge (the *body*), a rod of 0.32m length and 0.426kg weight, and an elastic and highly damping element made of adiPREN® with 0.028kg weight and a diameter of 35mm (the *foot*). For consistency with the CDSM model introduced in 2.1., the part of the rod below the body is called the *shank*. Upright rails force both body and shank to move in the vertical direction. A DC-motor (Maxon RE30 310007, with 3.7:1 gearhead Maxon GP 32 C 166930) fixed to the body actuates the shank (rod) via a rigid tooth belt and a tooth wheel (radius=19.5mm). The rotational inertia of the motor is, per data sheet,  $3.33 \cdot 10^{-6} \text{kg} \cdot \text{m}^2$ . An analogue power amplifier (Mattke MAR 24/12 ZE) operating in the voltage-to-current mode drives the motor. Hence, the current through amplifier and motor is proportional to the force  $F$  exerted from the motor to the shank. SIMULINK Realtime software (fixed step sample time 1ms, solver Dormand Prince (ode5) organizes

<sup>a</sup> The name “Marco” was given to the machine by Zully Ritter when she was staying in the Locomotion Lab.

through AD- and DA-conversion (interface: Meilhaus ME 2600) the control of the power amplifier. The ground reaction force  $f_g$  (GRF) is measured by a strain gauge (Megatron KM200). The friction between body and rail is very low and doesn't hamper the body's motion. Damping and friction exerted to the shank through the tooth belt and the wheel-gear-motor combination, however, are considerable: The coefficient of velocity dependent damping,  $b_1$ , was assessed as  $1.8\text{Ns/m} \pm 0.18$ , and the coefficient of friction force,  $c_1$ , was assessed as  $4.18\text{N} \pm 1.3$ , that is to say, these coefficients exhibited considerable fluctuation. The adiPREN foot diminishes the impacts at touch down and prevents the machine from damage at landing. Though the foot's material behaves non-linearly, rough values for stiffness and damping could be determined as  $k_2=15\text{kN/m}$ , and  $b_2=300\text{Ns/m}$ .

Before starting a hopping sequence, at first the shank's length was fixed to  $l_{10}=0.1\text{m}$ . Then the body, including shank and adiPREN foot, was lifted by hand, until the distance between ground and body reached the pre-selected release height  $y(0)$ . Releasing the body at this height initiated a bouncing sequence. The Poincaré apex return maps are shown in fig.2 (right column). They closely correspond to the return maps resulting from simulation, which are given in fig.2 (left column). Though minor differences are visible probably due to the non-adequate modeling of the non-linear adiPREN foot as a linear damped spring. We concluded that the machine's behavior validates the essential features of the CDSM concept. The Marco hopper's results can be interpreted in the same manner as outlined in the respective chapter 2.1: Lost energy supply produces something that resembles apex preserving hopping, but which is barely to stabilize, whereas constant energy supply generates terrain following hopping of high stability and robustness.

### 2.3 The behavioral comparison test

The behavioral comparison test requires contrasting experimental human data with adequately simulated data, where both data sets are generated under the same scenario (means equalized or matched parameters, conditions, boundaries etc). In the human hopping experiment, the subject starts a sequence of vertical jumps with both legs in parallel. Reflecting markers allow capturing the positions of hip, knee, ankle and foot via the camera system (QualiSys). The ground reaction force is measured by a force platform. A flat Styropor box of either 5cm or 10cm height laid upon the force platform provides the floor. In arbitrarily selected sequences the operator pulls after a few jumps the box away. So, the subject experiences a sudden step down of the floor, what is equivalent to an augmented release height. Hopping apices refer to the vertical motion of the center of mass (COM).

To get a preliminary impression of the results, fig.4 shows the trajectories of ground reaction force (GRF) and vertical movement generated by simulated, robotic and human hopping. Regarding the CDSM model, fig.4 suggests that lost energy supply approaches apex-preserving hopping when the floor is lowered. The CDSM model and the Marco hopper as well provide evidence that constant energy supply will lead to terrain following hopping. Qualitative comparisons of both kinds of trajectories to the respective human trajectories given in fig.4 reveal a considerable

resemblance with the terrain following hopping style. So it stands to reason that also the human hopper rather pursues terrain following hopping, but not apex preserving hopping. That humans apply constant energy supply to attain this type of bouncing seems, too, reasonable, but the verification must be left to further research.

Marco's needle shaped peak ground reaction forces at touch down (see Fig.4, 3<sup>rd</sup> row), however, do not fit well into these observations. They are caused by too large stiffness and damping parameters of the adiPREN ball taken as foot. Those peaks occur also in the simulated ground reaction forces when the Marco hopper's parameters are inserted into the CDSM model (not shown here).

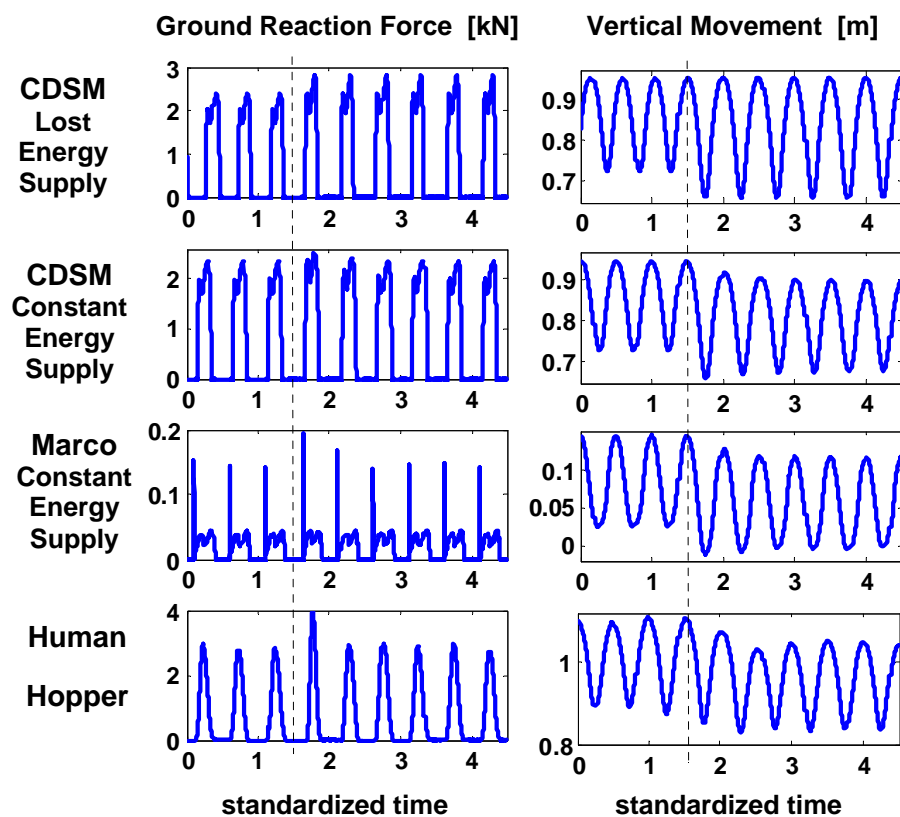


**Figure 4:** Ground reaction force (GRF) and vertical movement generated by the CDSM model and by the Marco hopper, under lost and constant energy supply. These trajectories are contrasted to the curves produced by a typical human hopper, which are shown in the last row. Time is standardized with respect to the length of the hopping cycles. The vertical dashed line indicates the point of time where the floor undergoes a sudden lowering (5cm in the CDSM model and in human hopping). Vertical movement refers to the y-coordinate of mass  $m_1$  in the CDSM model updated with human parameters, of the body in the Marco Hopper, and of the COM in the human hopper.



### 3 Discussion

The motivation underlying the presented paper is to pinpoint current research into hopping as focused too much on the energetically conservative mass-spring template. That inherently implicates apex-preserving hopping as hopping standard, even in human movement. Hopping research oriented onto this target commonly addresses energetic dissipation, if alluded to at all, as a kind of perturbation that hinders hopping to perpetuate or to achieve a desired height. Here we suggest replacing this approach with the damped spring-mass concept. This concept considers energetic dissipation not as a cumbersome perturbation, but as an appropriate tool that makes physical hopping enduring, and stabilizes it in a terrain following manner.

Terrain following hopping requires an energy management we call constant energy supply, whereby in each cycle the same amount of mechanical energy is injected, regardless of the current state of the hopper. The injected energy counterbalances the dissipative losses caused by damping and friction, such that the kinetic energy at takeoff converges on a constant value. This in turn determines the hopping height. So, the trajectories of body and leg are neither predefined nor enforced as in traditional control-theoretical approaches, but rather emerge from the physical properties of the leg. This type of “control” we call *exploitive actuation*<sup>2</sup>, which usually gets along with a minimum of computational effort. Apex preserving hopping, in contrast, would require lost energy supply that at best results in an unstable equilibrium. Even smallest external influences then suffice to drive hopping in to stall or build up.

Our preliminary results suggest that human hopping is closer to terrain following hopping respectively to constant energy supply than to apex preserving hopping. In human hopping, however, compliance is based on muscle-tendon elements that lack friction and exhibit only low structural damping. Does there exist a solution that guarantees energy losses high enough to produce robust and stable terrain following hopping? The intrinsic properties of the muscle as described in Hill-type muscle models<sup>10,11</sup> could provide an appropriate mechanism. Such a mechanism would make hopping less sensitive to internal perturbations like fluctuations of muscular activation, or external disturbances like changed ground properties, all without to occupy “cognitive resources”. There exists in deed evidence that the Hill-type combination of force-length and force-velocity relationships of muscles provides an effective reduction of sudden perturbations<sup>12-15</sup>, and even enables stable hopping<sup>16</sup>. Further behavioral comparison tests in the framework of the test trilogy are in preparation. The outcome of the tests might answer some of the questions.

**Acknowledgements** We thank for support by grants SE1042/2 and KA417/24 from the German Research Foundation (DFG).

## References

1. Blickhan, R. The spring-mass model for running and hopping. *Journal of Biomechanics* **22**, 1217-1227 (1989).
2. Kalveram, K. T. & Seyfarth, A. Inverse biomimetics: How robots can help to verify concepts concerning sensorimotor control of human arm and leg movements. *Journal of Physiology - Paris* **103**, 232-243 (2009).
3. Kalveram, K. T., Schinauer, T., Beirle, S., Richter, S. & Jansen-Osmann, P. Threading neural feedforward into a mechanical spring: How biology exploits physics in limb control. *Biological Cybernetics* **92**, 229-240 (2005).
4. Raibert, M. H. Hopping in legged systems---Modeling and simulation for the 2D one-legged case. *IEEE Transactions on Systems, Man, and Cybernetics* **14**, 451-463 (1984).
5. Rad, H., Gregorio, P. & Buehler, M. in *Proceedings of the IEEE/RSJ Conference on Intelligent Robots and Systems* 1778-1785 (Yokohama, Japan, 1993).
6. Pelc, E. H., Daley, M. A. & Ferris, D. P. Resonant hopping of a robot controlled by an artificial neural oscillator. *Bioinspiration and Biomimetics* **3**, 026001 (2008).
7. Guckenheimer, J. & Holmes, P. *Nonlinear Oscillations, Dynamical Systems and Bifurcations of Vector Fields* (Springer, New York, 2002).
8. Rummel, J. & Seyfarth, A. Stable Running with Segmented Legs. *The International Journal of Robotics Research* **27**, 919-934 (2008).
9. Seyfarth, A., Kalveram, K. T. & Geyer, H. in *Autonome Mobile Systeme* (eds. Berns, K. & Luksch, T.) 294-300 (Kaiserslautern, Germany, 2007).
10. Winters, J. M. in *Multiple muscle systems: biomechanics and movement organization* (eds. Winters, J. M. & Woo, S. Y.) 69-93 (Springer, New York, 1990).
11. Winters, J. M. An improved muscle-reflex actuator for use in large-scale neuromusculoskeletal models. *Annals of Biomedical Engineering* **23**, 359-374 (1995).
12. van Soest, A. J. & Bobbert, M. F. The contribution of muscle properties in the control of explosive movements. *Biological Cybernetics* **69**, 195-204 (1993).
13. Gerritsen, K., van den Bogert, A., Hulliger, M. & Zernicke, R. Intrinsic muscle properties facilitate locomotor control-a computer simulation study. *Motor Control* **2**, 206 (1998).
14. Geyer, H., Seyfarth, A. & Blickhan, R. Positive force feedback in bouncing gaits? *Proceedings of the Royal Society of London Series B - Biological Sciences* **270**, 2173-2183 (2003).
15. Wagner, H. & Blickhan, R. Stabilizing function of skeletal muscles: an analytical investigation. *Journal of Theoretical Biology* **199**, 163-179 (1999).
16. Haeufle, D. F. B., Grimmer, S. & Seyfarth, A. The role of intrinsic muscle properties for stable hopping - stability is achieved by the force - velocity relation. *Bioinspiration & Biomimetics* **5/016004**, doi: 10.1088/1748-3182/5/1/016004 (2010).